Molecular Nutrition & Food Research
www.mnf-journal.com

AKT1/HK2 Axis-mediated Glucose Metabolism: A Novel Therapeutic Target of Sulforaphane in Bladder Cancer

Lei Huang, Canxia He, Sicong Zheng, Chao Wu, Minghua Ren, and Yujuan Shan**

Scope: Metabolic disorder is a pivotal hallmark of cancer cells. Sulforaphane (SFN) is reported to improve lipid metabolism. However, the effect of SFN on glucose metabolism in bladder cancer remains unclear. Hence, the effect and underling mechanism is investigated.

Methods and Results: Biological samples from bladder cancer patients are collected, and also investigated using N-butyl-N-(4-hydroxybutyl) nitrosamine-induced bladder cancer mice and bladder cancer cell lines. A novel glucose transport aberrant-independent aerobic glycolysis is found in bladder cancer patients, and the lower malignancy tissues have the more obvious abnormality. SFN strongly downregulates ATP production by inhibiting glycolysis and mitochondrial oxidative phosphorylation (OXPHOS). Both in vitro cell culture and in bladder tumor mice, SFN weaken the glycolytic flux by suppressing multiple metabolic enzymes, including hexokinase 2 (HK2) and pyruvate dehydrogenase (PDH). Moreover, SFN decreases the level of AKT1 and p-AKT ^{ser473}, especially in low-invasive UMUC3 cells. The downregulation of ATP and HK2 by SFN is both reversed by AKT1 overexpression.

Conclusions: SFN downregulates the unique glucose transport aberrant-independent aerobic glycolysis existed in bladder cancer via blocking the AKT1/HK2 axis and PDH expression.

1. Introduction

Sulforaphane (SFN) is an isothiocyanate (ITC) derived from cruciferous vegetables and has been proven to be a powerful prospect against various tumors,[1] including colon cancer,[2] breast cancer,[3] and bladder cancer.[4] Ingested SFN are mainly metabolized through the mercapturic acid pathway.[5] SFN metabolites were able to stay in bladder at relative higher concentrations and for longer periods,[6] which implied more powerful and potential roles on targeting against bladder cancer. A follow-up trial involving 239 bladder cancer patients for eight years found a significant increase of survival rates in patients who consumed broccoli per month.[7] Other epidemiological studies also showed that dietary consumption of ITCs was inversely correlated with the risk of developing lung, breast and colon cancers.[8] We previously demonstrated that SFN blocked bladder cancer cell invasion by reversing epithelial-to-mesenchymal transition process via directly targeting the microRNA-200c/Zinc finger E-box-binding protein (ZEB1) axis.[9] Furthermore, cyclooxygenase-2 overexpression largely reversed the inhibition of matrix metalloproteinase (MMP) 2/9 by SFN, thereby abolishing bladder cancer cell invasive suppression.[10]

It is famously known that energy metabolism plays an important role in affecting tumors metastasis,[11] meanwhile metastasis is one of the leading causes of bladder cancer-associated poor prognosis and high mortality.[12] Just as people cannot walk without energy, adequate energy is essential for tumor growth and migration.[13] Therefore, targeted energy metabolism may have great potential in exploring bladder cancer metastasis. Various studies on the metabolic profiles have found that severe glucose metabolic disorders exist in bladder cancer (urine,[14] serum,[15] and cell lines[16]), however, the systemic metabolic profile is still unclear. According to our previous results, SFN promoted mitochondrial biogenesis and function through enhancing lipids utilization in human liver cells.[17] Furthermore, we also found SFN can regulate abnormal lipid metabolism in human hepatocytes,[18] suggesting that SFN may be involved in the regulation of cell energy metabolism. To our knowledge, the effect and mechanism of

L. Huang, S. Zheng, C. Wu, Y. Shan
School of Public Health and Management
Wenzhou Medical University
Wenzhou 325000, China
E-mail: yujuanshan@wmu.edu.cn
L. Huang
Department of Medicine
Brigham and Women's Hospital, Harvard Medical School
Boston, MA 02139, USA
C. He
Institute of Preventative Medicine and Zhejiang Provincial Key Laboratory of Pathological and Physiological Technology, School of Medicine
Ningbo University
Ningbo 315211, China
M. Ren
Department of Urology
The First Affiliated Hospital of Harbin Medical University
Harbin 150001, China
E-mail: renminghua@163.com

The ORCID identification number(s) for the author(s) of this article can be found under https://doi.org/10.1002/mnfr.202100738

DOI: 10.1002/mnfr.202100738

SFN on bladder cancer cells metabolism are still required to be clarified.

In this study, we showed a novel characteristic of glucose transport aberrant-independent aerobic glycolysis in bladder cancer patients, and the lower malignancy tissues have the more obvious abnormality. SFN can downregulate glycolysis and mitochondrial OXPHOS via blocking the AKT1/HK2 axis and PDH expression, respectively.

2. Experimental Section

2.1. Reagents

D,L-Sulforaphane (1-isothiocyanato-4-methylsulphinylbutane, purity ≥ 98%) was purchased from LKT Laboratory (St. Paul, MN), dissolved in dimethyl sulfoxide (DMSO, stored at −20°C). N-Butyl-N-(4-hydroxybutyl) nitrosamine (BBN) was purchased from Sigma-Aldrich. The antibodies against HK2, PKM2, PDH, AKT1, p-AKT, and GAPDH were all purchased from Protein-tech (Chicago, USA).

2.2. Patients and Sample Collection

All experiments involving humans have been carried out in accordance with the Code of Ethics of the World Medical Association and informed consent was obtained for human subjects. The protocol was approved by the Ethics Committee of the First Affiliated Hospital of Harbin Medical University and registered at www.chictr.org.cn as ChiCTR-OOC-16007937. To investigate the metabolic characteristics of bladder cancer patients, patients were recruited at the First Affiliated Hospital of Harbin Medical University. All the diagnoses of bladder cancer patients who with no other tumor history and metabolic disease were confirmed by cystoscopy examinations. Thirty-three cases of bladder tumor and twenty adjacent non-tumor tissue samples were collected from patients undergoing surgical resection. Tumors were characterized into low-muscle invasive (≤ T1 grade) cancer without subsequent stage progression and high-muscle invasive (≥T2 grade) with local or distant metastasis. The specimens were immediately frozen in liquid nitrogen and then stored at −80°C. Blood samples were obtained from 31 bladder cancer patients and from 46 healthy subjects who visited for physical examinations. About 5 mL of blood was drawn from participants and clotted for 2 h at room temperature. Then the serum was separated after centrifugation at 3000 rpm for 10 min and stored at −80°C. Table S1 (Supporting Information) summarizes all the clinicopathological data of all the patients.

2.3. GC-MS Analysis of Metabolites

The human bladder tumor tissues were stored at −80°C before GC-MS targeted analysis. Tissues were resuspended in 0.4 mL cold (-20°C) 50% aqueous methanol containing 100 µM norvaline as an internal standard, frozen on dry ice for 30 min, then thawed on ice for 10 min before centrifugation. The supernatant was then partitioned with 0.3 mL chloroform to reduce the fatty acid content. The methanol fraction was dried by centrifugal evaporation and stored at -80°C before analysis. Metabolites were derivatized for GC/MS analysis as follows: first, 50 µL of 20 mg mL^{-1} O-Isobutyl hydroxylamine Hydrochloride (TCI) was added to the dried pellet and incubated for 20 min at 80°C. After cooling, 50 µL of N-tert-butyldimethylsilyl-N-methyltrifluoroacetamide (Sigma) was added and samples were reincubated for 60 min at 80°C before centrifugation for 5 min at 14 000 rpm (4°C). The supernatant was transferred to an autosampler vial for GC/MS analysis. A Shimadzu QP-2010 Ultra GC-MS was programmed with an injection temperature of 250°C injection split ratio 1/10 and injected with 1 µL of sample. GC oven temperature started at 110°C for 4 min, rising to 230°C at 3°C min^{-1} and to 280°C at 20°C min^{-1} with a final hold at this temperature for 2 min. GC flow rate with helium carrier gas was 50 cm s^{-1}. The GC column used was a 30 m × 0.25 mm × 0.25 mm HP-5ms. GC-MS interface temperature was 300°C and (electron impact) ion source temperature was set at 200°C, with 70 V/150 µA ionization voltage/current. The mass spectrometer was set to scan m/z range 50–800, with 1 kV detector. GC/MS data were analyzed to determine isotope labeling and quantities of metabolites. Metabolites with baseline separated peaks were quantified based on total ion count peak area, using standard curves generated from running standards in the same batch of samples.

2.4. BBN-induced Bladder Tumor Model in C57BL/6 Mice

Male C57BL/6 mice (5 weeks old, 16–20 g in body weight, specific pathogen free) were maintained with free access to pellet food and water in solid-bottom cages that contained a bedding of softwood shavings at 22 ± 2°C with a humidity of 55 ± 5% and a 12 h light-dark cycle. The schematic diagram descripted the entire animal experiment process (Figure 5A). Animal welfare and experimental procedures were performed strictly in accordance with the guidelines of the U.K. Animals (Scientific Procedures) Act, 1986. The protocol was approved by the Ethic Committee of Experimental Animals.

Dose information: Male C57BL/6 mice were treated with different doses of SFN (2.5, 5, and 10 mg kg^{-1}) by oral gavage three times a week for 23 weeks (Figure 5A). According to the published literature,[19,20] mice received 0.05% (w/v) BBN in the drinking water for 12 weeks to induce bladder carcinogenesis.

2.5. Cell Culture and Transfection

Human bladder cancer cell lines (RT4: transitional cell papilloma, T24: pathology grade 3, UMUC-3: pathology grade 1) were kindly provided by Prof. Yuesheng Zhang (Roswell Cancer Institute, USA). Human umbilical vein endothelial cell (HUVECs) was stored at our laboratory. Cells were grown at 37°C in a humidified incubator with 5% CO_2. For transient transfection, cells were seeded to 70–90% confluence. Lipofectamine reagent (Thermo Fisher Scientific, MA, USA) and p $^{EGFP\ n\text{-}1\ AKT1}$ (Sangon Biotech, Shanghai, China) were diluted in Opti-MEM medium at 8% and 2% concentrations, respectively, and then mixed at a ratio of 1:1. After incubating for 5 minutes at room temperature, the DNA-lipid complex was added to cells and incubated for 24 h at 37°C. Cells were harvested before experiments.

Dose information: After reaching 70% confluence, bladder cancer cells were treated with different doses of SFN (1, 5, 10, 20 μmol L^{-1}) for 24 h.

2.6. Bioenergetic Function Analysis

The bioenergetic metabolism of bladder cancer cells were measured using a XFp Extracellular Flux Analyzer (Seahorse Bioscience, North Billerica, MA, USA). Cells seeded in XFp 8 well microplates at 2×10^3 cells $well^{-1}$ were incubated at 37°C for 3 h. Then, the cells were treated with different concentrations of SFN. One hour before measurement, culture medium was replaced by assay medium, then the values of the oxygen consumption rate (OCR) and extracellular acidification rate (ECAR) were measured with the XFp Extracellular Flux Analyzer before and after the injection of 1 μM oligomycin, 2 μM FCCP, 0.5 μM rotenone, and 1 μM antimycin.

2.7. Measurement of Metabolic Enzyme Activities

The activities of metabolic enzymes (HK2, PKM2, and PDH) in the serum of bladder cancer patients and bladder cancer cells were detected using commercially available kits (Keming, Jiangsu, China) according to the manufacturers' instructions.

2.8. ATP Content Assays

The intracellular ATP level was measured by the Luminescent ATP Detection Assay (Promega, Madison, USA). After SFN treatment for 24 h, 100 μL of reagent was added to 100 μL of medium in each well to release the intracellular ATP. The plate was incubated at room temperature for 10 min to stabilize the luminescence signal, and the luminescence intensity was measured using microplate reader (TECAN Infinite200 PRO).

2.9. Real-time Quantitative Polymerase Chain Reaction Analysis

Total RNA was extracted from cells and tumor tissues with a TRIzol RNA isolation kit (Invitrogen, Grand Island, NY, USA). RNA concentration and purity were measured using a Nanodrop Spectrophotometer (Labtech International, UK). cDNA was synthesized from purified RNA using a cDNA Synthesis Supermix Kit (TransGen Biotech, Beijing, China) as described in the manufacturer's manual. The primers for humans and mice are shown in Table S2 and Table S3 (Supporting Information), respectively. The comparative cycle threshold ($2^{-\Delta\Delta Ct}$) method was used to evaluate the relative gene transcript levels, normalized to the β-actin reference gene. The data represent the average of three independent experiments from three biological replicates per experiment.

2.10. Western Blot Analysis

Whole protein and nucleoprotein lysates were prepared according to the previous instructions.[9] An equal amount of protein was separated by SDS-PAGE and transferred onto PVDF membranes. After 4°C overnight incubation with specific primary antibodies—including those against HK2 (1:2000), PDH (1:1000), PKM2 (1:1000), AKT1 (1:2000), p-AKT1 (1:2000), and GAPDH (1:6000)—the membranes were then incubated with the secondary antibody (1:3000) at room temperature for 1 h. The protein signals were visualized by a chemiluminescence detection kit (Solarbio, Beijing, China).

2.11. Immunohistochemistry Measurement

Immunohistochemical assays were performed using an anti-rat/rabbit General Immunohistochemical Test Kit (Proteintech, Chicago, USA) according to the manufacturer's instructions. Paraffin-embedded bladder sections were de-paraffinized and rehydrated. Heat-induced epitope retrieval was performed using a citrate antigen retrieval solution for 5 min. Endogenous peroxidase activity was blocked by incubating with 0.3% H_2O_2 for 15 min. Overnight incubation was performed at 4°C with specific primary antibodies, including those against HK2 (1:200), PKM2 (1:100), PDH (1:200), and AKT (1:100). Immunolabeled sections were examined by light microscopy.

2.12. Statistical Analysis

Data were expressed as mean ± SD. Statistical analysis was performed using unpaired Student's *t*-tests or one-way or two-way ANOVA. Quantification of protein expression was measured using the ImageJ software (NIH, USA). The results were analyzed using the GraphPad Prism Software version 7.0 (GraphPad Software Inc., San Diego, CA, USA). The values in all figures are statistically significant at $p < 0.05$.

3. Results

3.1. Distinguishing Features of Glucose Metabolism in Bladder Cancer Patients

To investigate the characteristics of glucose metabolism in patients with bladder cancer, we collected tumor tissues at different tumor lymph node metastasis (TNM) stages and measured the contents of glucose-related metabolites (**Figure 1A**) by Gas Chromatography-Mass Spectrometry (GC-MS). The heat map result showed that most glucose metabolites were highly expressed in bladder tumors compared with the para-carcinoma tissues (Figure 1B, left panel). The variation of metabolites arranged by unsupervised hierarchical clustering revealed the distinguished clusters between para-carcinoma tissues and tumor tissues (Figure 1B, right panel). The level of ATP in bladder tumors was significantly increased by 16.6 times (Figure 1C), suggesting that ATP production capacity was extremely strengthened in tumor tissues, especially in low-muscle invasive tissues (T1 stage; Figure S1A, Supporting Information). Glucose intake was not significantly different (Figure 1D and Figure S1B, Supporting Information), although lactate production in the tumor tissue was 2.7 times higher than that in the adjacent tissue (Figure 1D and Figure S1C, Supporting Information). Furthermore, glucose-6-phosphate (G-6-P, a product of glucose catalyzed by HK2) was the

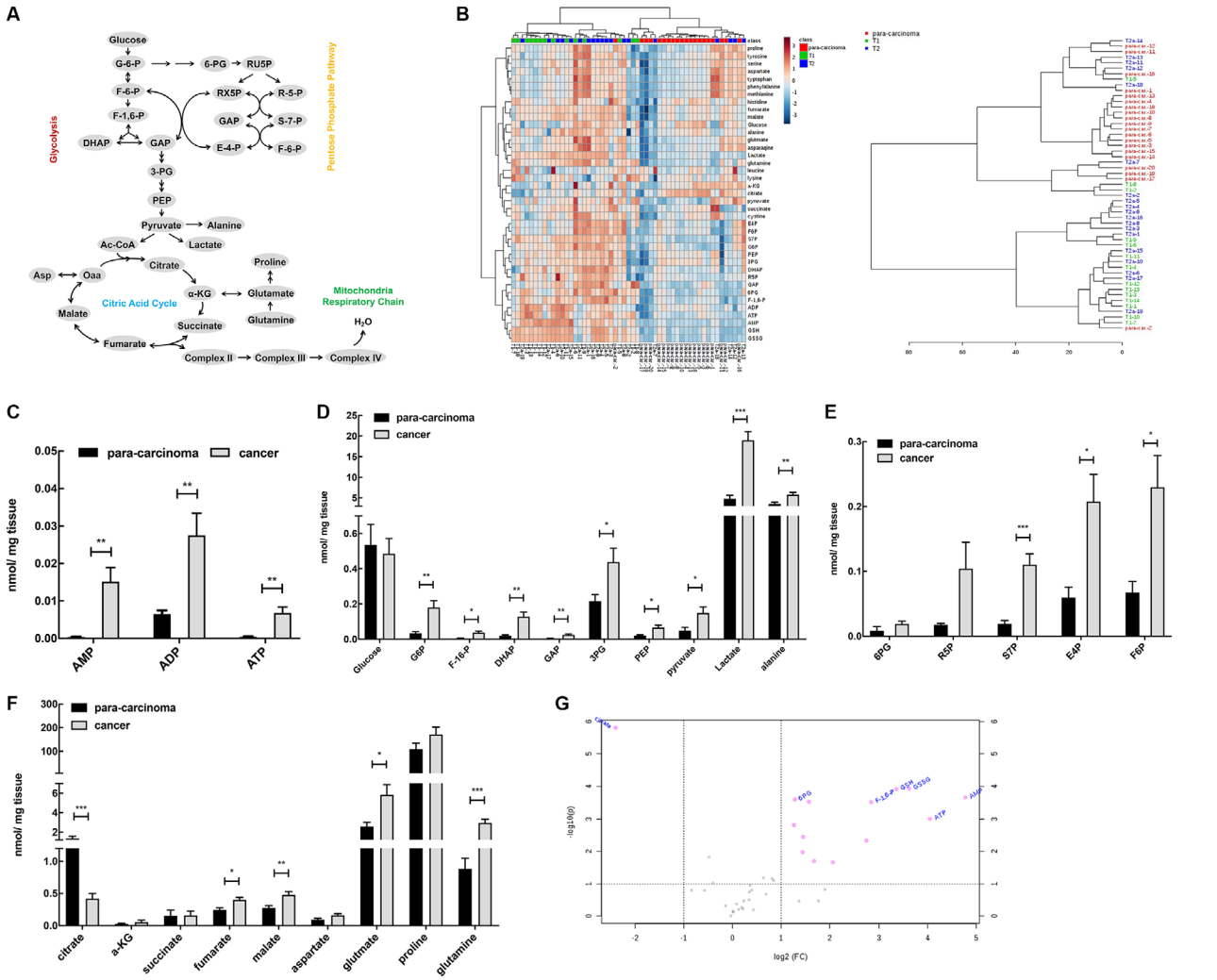

Figure 1. Distinguishing features of glucose metabolism in bladder cancer patients. A) Schematic depicting the profile of intracellular glucose metabolism. B) GC-MS analyses demonstrating the changes of 39 glucose metabolites in bladder tissues. The right panel shows the variation of metabolites from para-carcinoma and tumor tissues arranged by unsupervised hierarchical clustering in 53 samples. C) The contents of ATP, ADP and AMP in bladder tissues were detected by GC-MS. D-F) The changes of metabolites in glycolysis (D), pentose phosphate pathway (E) and tricarboxylic acid cycle (F) between tumor and para-carcinoma tissues. G) The volcano plot analysis of the fold changes of glucose metabolites. All data were analyzed using unpaired *t* tests. Compared with the para-carcinoma group, $^{*}p < 0.05$, $^{**}p < 0.01$, $^{***}p < 0.001$.

first metabolite significantly upregulated in the glycolysis process (Figure 1D and Figure S1D, Supporting Information), suggesting the increased utilization of glucose, but not the uptake by bladder cancer cells.

To corroborate the profile of glucose metabolism, we further analyzed the metabolites of pentose phosphate pathway (PPP) and tricarboxylic acid (TCA) cycle (Figure 1A). Many metabolic intermediates including sedoheptulose 7-phosphate (S7P), erythrose 4-phosphate (E4P) and fructose-6-phosphate (F6P) were highly expressed in tumor tissues (Figure 1E). Similarly, TCA cycle was extremely active and as a main intermediate metabolite, citrate was found to be obviously decreased in bladder tumors (Figure 1F), especially in T1 stage tissue (Figure S1E, Supporting Information). Succinate dehydrogenase (SDH) catalyzes the oxidation of succinate into fumarate and then participates in the mitochondrial electron transport chain (mETC). However, the sudden increase of fumarate but not succinate indicated that the SDH-catalyzed reaction (allowing H^+ to enter mETC to produce abundant ATP) may be disturbed in bladder tumors (Figure 1F). The Volcano Plot analysis revealed that 14 glucose metabolites were differentially expressed (Figure 1G, pink points), and among which 13 metabolites were upregulated by more than two-fold ($p < 0.05$). To our knowledge, the current data maybe firstly show a distinguishing "Warburg effect"[24] in bladder cancer, where the hyperactivity of glucose metabolism may not be mainly caused by excessive glucose uptake.

3.2. Upregulation of Glucose Metabolism-related Enzymes

To further validate the major factors stimulating the hyperactivity of glucose metabolism in patients, we examined the activity

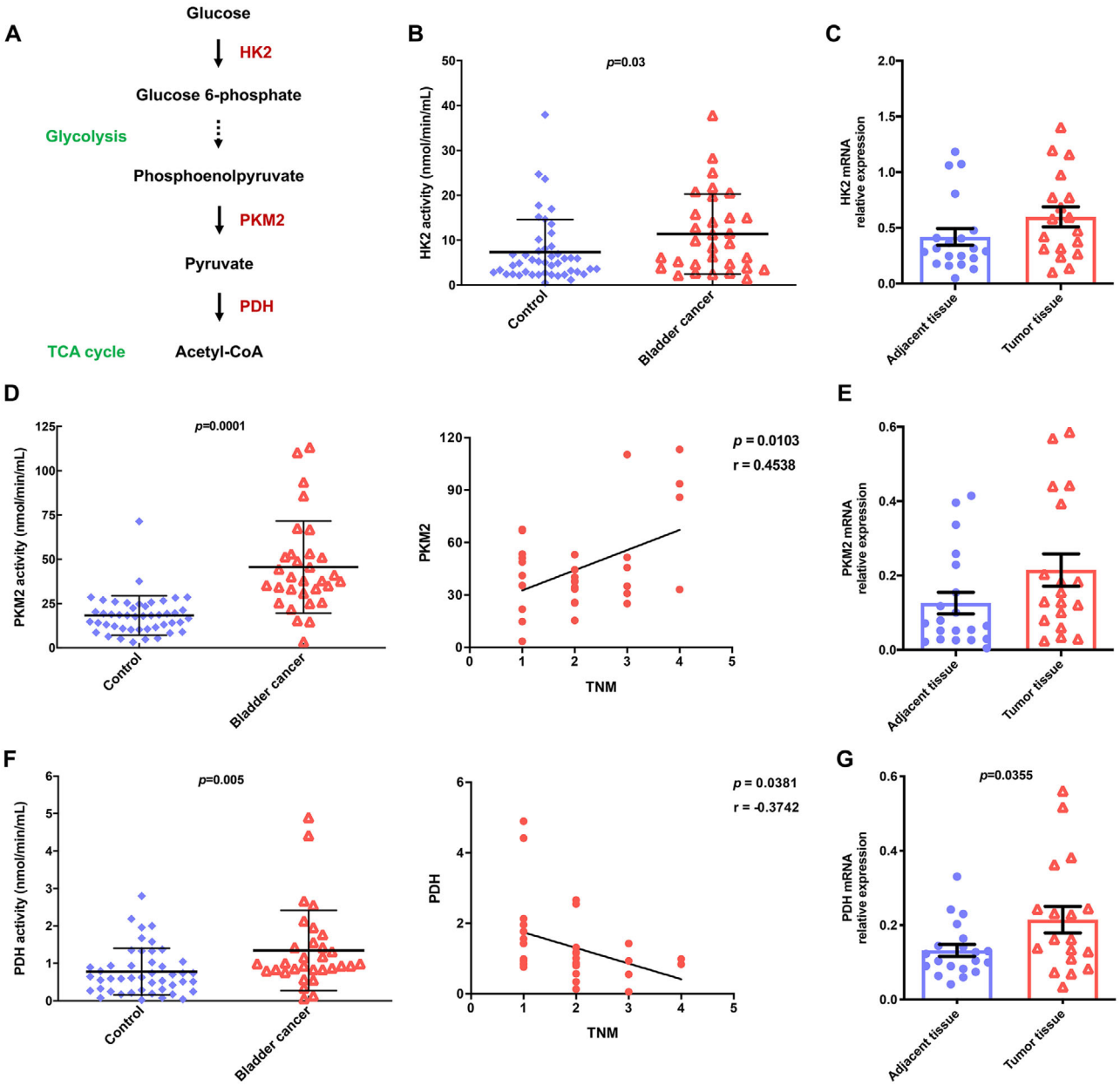

Figure 2. Upregulation of glucose metabolism-related enzymes. A) Key enzymes in glycolysis. B, C) The serum activity (B) and mRNA level (C) of HK2 in bladder cancer patients. D) The serum activity of PKM2 (left panel) and correlation analysis (right panel) with TNM staging. E) The mRNA level of PKM2 in bladder tumor tissues. F) The serum activity of PDH (left panel) and correlation analysis (right panel) with TNM staging. G) The mRNA level of PDH in bladder tumor tissues. All data were analyzed using unpaired *t* tests. Pearson rank correlation was used for correlation tests.

of key metabolic enzymes (**Figure 2A**). Abnormal activation of HK2 activity was observed in patients (Figure 2B), but not in the mRNA level (Figure 2C). PKM2, as the last rate-limiting enzyme catalyzes the production of pyruvate, was significantly increased in patients (Figure 2D left panel) and positively correlated with TNM stage ($r = 0.4538$, $p = 0.01$; Figure 2D right panel); meanwhile no significance in the mRNA level (Figure 2E). Of note, the activity ($p = 0.005$; Figure 2F left panel) and mRNA level (Figure 2G) of PDH were significantly elevated in patients, and the former was negatively correlated with TNM stage ($r = -0.3742$, $p = 0.03$; Figure 2F right panel).

3.3. SFN Inhibited ATP Production by Downregulating Both Glycolysis and Mitochondrial Oxidative Phosphorylation

It is well known that cells mainly utilize carbohydrates for energy supply by two pathways, namely glycolysis and mitochondrial OXPHOS (**Figure 3A**). Two kinds of bladder cancer cell lines with different pathological grades (T1 grade: UMUC3, T3 grade: T24) were chose to examine ATP production, using HUVECs as a negative control. As shown in Figure 3B, the level of ATP in bladder cancer cells was significantly higher than that in HUVECs ($p < 0.001$), and SFN inhibited ATP production in a

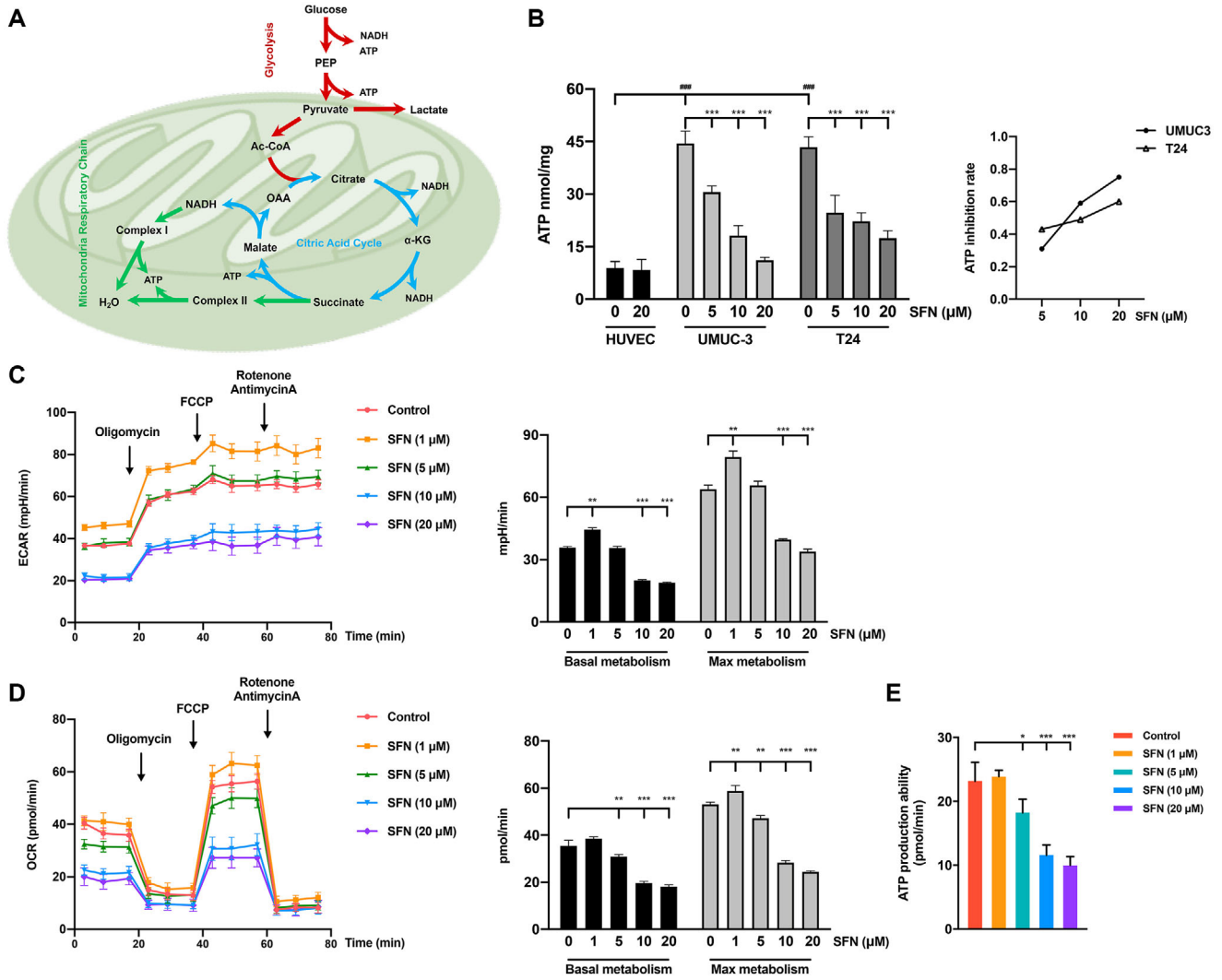

Figure 3. SFN inhibited ATP production by downregulating both glycolysis and mitochondrial oxidative phosphorylation. A) Schematic diagram showing the process of glucose metabolism and ATP produced by mitochondria and glycolysis. B) ATP levels in different groups. The inhibition rate is shown in the right panel. ECAR (C) and OCR (D) were detected by extracellular flux analysis; the right panels were basal and max metabolism. E) Maximum capacity of ATP production. Compared with the control group, $^{*}p < 0.05$, $^{**}p < 0.01$, $^{***}p < 0.001$; Compared with the HUVEC negative control group, $^{###}p < 0.001$.

dose-dependent manner but not in HUVECs. Of note, much stronger inhibition in ATP production was found in UMUC3 cells (Figure 3B right panel), combined with more significant upregulation level of ATP in T1 stage tissues (Figure S1A, Supporting Information), indicating the potential of SFN in improving the metabolic disorders especially with low-invasive bladder cancer patients.

Next, to further corroborate how SFN suppresses the energy supply, we measured the bioenergetic profile oxygen consumption rate (OCR; OXPHOS capacity) and extracellular acidification rate (ECAR; glycolysis capacity) using a Flux analyzer. SFN decreased ECAR in a dose-dependent manner (Figure 3C left panel), meanwhile, 20 μmol L^{-1} SFN exhibited the strongest inhibition on both basal and maximum metabolic ability (Figure 3C right panel). In the same way, SFN powerfully inhibited mitochondrial OXPHOS (Figure 3D). After incubation with 20 μmol L^{-1} SFN for 24 h, ATP production ability was dramatically suppressed by 55.86% in T24 cells (Figure 3E). Together, these results suggested that SFN disrupted both glycolysis and mitochondrial OXPHOS in a dose-dependent manner, especially in UMUC3 cells, and thereby effectively suppressed ATP production.

3.4. SFN Inhibited Multiple Glucose Metabolic Enzymes in Invasive Bladder Cancer Cells

As Figure 2 concluded, the dysfunction of metabolic enzymes is the main reason of hyperactive glucose metabolism in bladder cancer patients. Thus, we subsequently investigated the effects of SFN on key glycolytic enzymes in vitro. SFN (20 μmol L^{-1}) significantly suppressed the mRNA levels (**Figure 4A**) and the activities (Figure 4B) of HK2 and PDH, whereas only HK2 activity

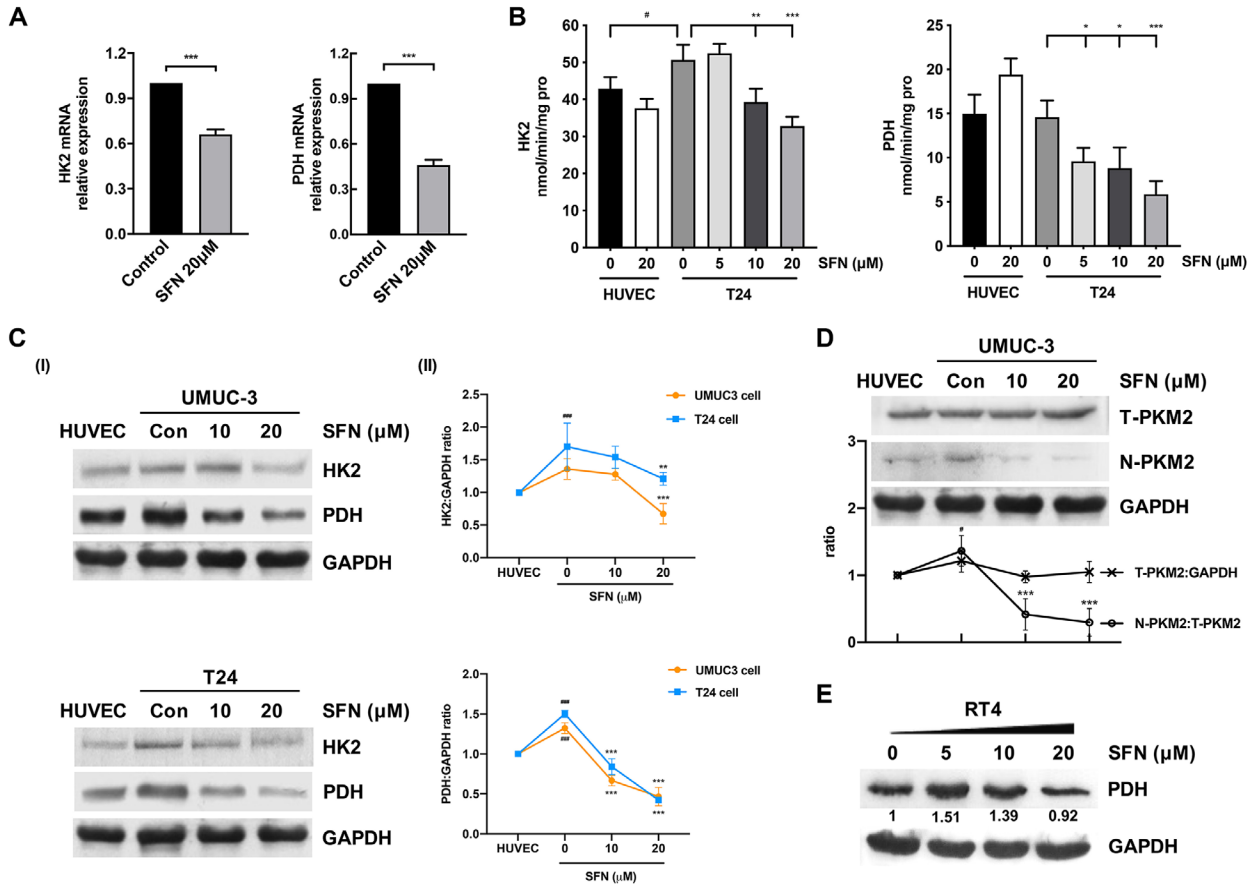

Figure 4. SFN inhibited multiple glucose metabolic enzymes in invasive bladder cancer cells. A) The mRNA level of HK2 and PDH in T24 cells. B) The activity of enzymes involved in glucose metabolism. C-I) Western blot analysis of HK2 and PDH; C-II) The relative densities of the target proteins. D) The protein level of total PKM2 (T-PKM2) and nuclear PKM2 (N-PKM2) in UMUC-3 cells, and quantification at the bottom. E) Western blot analysis of PDH in noninvasive RT4 cells. Compared with the control group, $^{*}p < 0.05$, $^{**}p < 0.01$, $^{***}p < 0.001$; Compared with the HUVEC negative control group, $^{\#}p < 0.05$, $^{\#\#\#}p < 0.001$.

was increased compared with HUVECs (Figure 4B), suggesting its leading role in the dysregulation of glucose metabolism. We also observed a significant reduction in the HK2 protein level upon SFN treatment in both cell lines (Figure 4C-I), and more powerful inhibition in UMUC3 cells (Figure 4C-II upper). Similarly, SFN decreased PDH protein expression (Figure 4C-I), and a slight stronger inhibition in T24 cells (Figure 4C-II lower). In addition, SFN inhibited nuclear level of PKM2 (N-PKM2) protein but not total PKM2 (T-PKM2) (Figure 4D). We also validated these enzymes in RT4 cells (highly differentiated transitional cell papilloma) and found that SFN hardly affected their protein expression (Figure 4E). These data revealed that the inhibitory effect of SFN on the glucose metabolism varied with the different pathological grades and was stronger in muscle invasive bladder tumors.

3.5. SFN Improved the Aberrant of Glucose Metabolism in BBN-induced Bladder Tumor Mice

Next, we further explored the impact of SFN on glucose metabolism in vivo using a BBN-induced bladder tumor mouse (**Figure 5A**). No significance was found in body weight during the whole experiment (Figure 5B). Bladder weights were increased in the BC group and low-dose SFN group (Figure 5C). The protein and gene expressions of HK2, PKM2, and PDH were downregulated by SFN (Figure 5D and E). Consistent with the enzyme activity (Figure 4B), the expression of HK2 mRNA was extremely high in BC group (Figure 5E). Together, these results demonstrated that SFN reversed the dysregulation of the glycolytic flux by inhibiting key metabolic enzymes both in vivo and in vitro.

3.6. SFN Reversed the Dysregulation of Glycolysis via the AKT1-HK2 Axis

To our knowledge, the underling mechanisms by which SFN regulated glycolysis in bladder cancer are rarely known. Previous evidence suggested that PI3K/AKT signaling pathway was closely associated with the regulation of aerobic glycolysis.[21,22] As compared with HUVECs, AKT1 protein is abnormally activated in T24 cells, especially the phospho-AKT^{Ser473} (p-AKT^{Ser473}) (Figure 6A). After incubation with 20 μmol L^{-1} SFN, AKT1, and p-AKT^{Ser473} were both suppressed (Figure 6A),

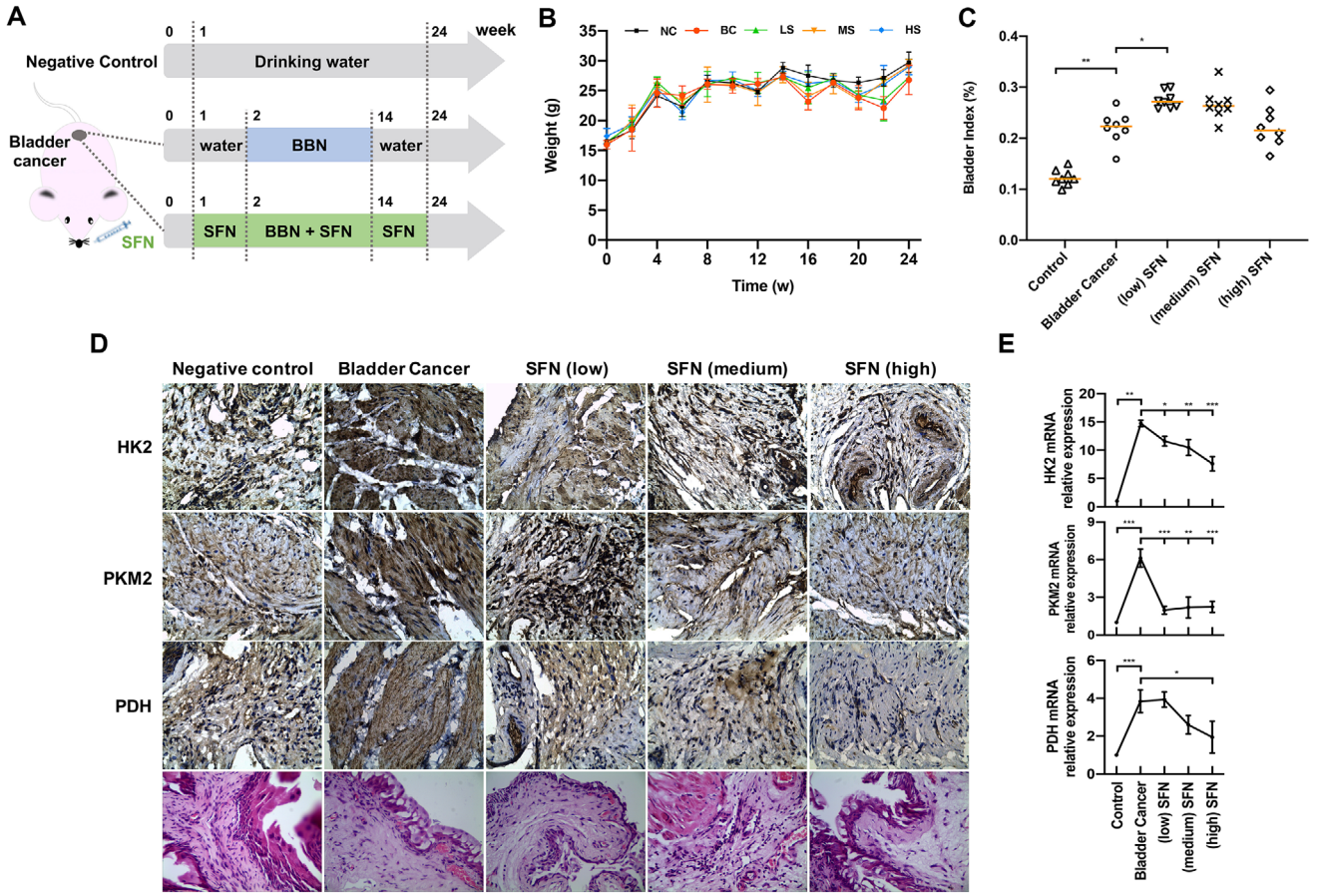

Figure 5. SFN inhibited multiple glucose metabolic enzymes in invasive bladder cancer cells. A) Schematic diagram descripting the animal experiment process. B) Body weight of mice during the whole experiment. C) Bladder index following SFN administration by oral at designed doses for 23 weeks. D) Representative images of immunohistochemical and H&E staining in bladder sections (× 100 magnification). E) The mRNA levels of glucose metabolic enzymes in bladder tissues. Compared with the BC group, $^{*}p < 0.05$, $^{**}p < 0.01$, $^{***}p < 0.001$.

suggesting that SFN could strongly block the activation of AKT1. Consistently, we observed a strong reduction of AKT1 both in the mRNA and protein levels in the HS-treated mice (Figure 6B).

To further determine whether the inhibitory effect of SFN on HK2 was mediated by AKT1, the overexpressed $p^{EGFP\text{-}n\text{-}1\ AKT1}$ was transfected into bladder cancer cells. As shown in Figure 6C, the decreased protein level of HK2 by SFN was strongly reversed by AKT1 overexpression. Also, the inhibitory effects of SFN on HK2 activity (Figure 6D) and ATP production (Figure 6E) were both disappeared in AKT1-overexpressing T24 cells. Taken together, these data implied that SFN reversed the dysregulation of glucose metabolism by inhibiting the AKT1-HK2 axis.

4. Discussion

Here, we showed a unique characteristic of glucose transport aberrant-independent aerobic glycolysis in bladder cancer patients, and the lower malignancy tissues have the more obvious abnormality. Moreover, SFN significantly downregulated glycolysis and mitochondrial OXPHOS via blocking the AKT1/HK2 axis and PDH expression (Figure 6F), which identifying a vital role of SFN in improving metabolic disorders in bladder cancer.

Cancers differed in the metabolic phenotypes, with aerobic glycolysis being one of the most common types of metabolic reprogramming.[23] The yield rate of ATP by glycolysis is much faster than mitochondrial OXPHOS. One of the main reasons is an avidly enhanced rate of glucose uptake, a pre-glycolysis step mediated by glucose transporters.[24] Inconsistently, the level of glucose in bladder tumor was not significantly higher than that in para-cancer tissues, yet the content of G-6-P catalyzed by HK2 was aberrantly increased. Thus, we surmised that the overactive HK2 was the main contributor to the dysregulation of glucose metabolism in bladder cancer. Also, the negative correlation between PDH activity and TNM stage indicated the higher OXPHOS level in low-grade tumors. These findings demonstrated that the glucose metabolism characteristics were different in patients with the different pathological stages and highlighted a major role for mitochondrial OXPHOS in early phases of carcinogenesis.

An adequate ATP supply is essential for the infinite proliferation of tumor cells.[25] Therefore, reversing the dysregulation of tumor metabolism could be utilized as an effective cancer therapy strategy. An increasing number of molecular targets have been considered as leading regulators of metabolism in different cancers. As the first rate-limiting enzyme in glycolysis, HK2

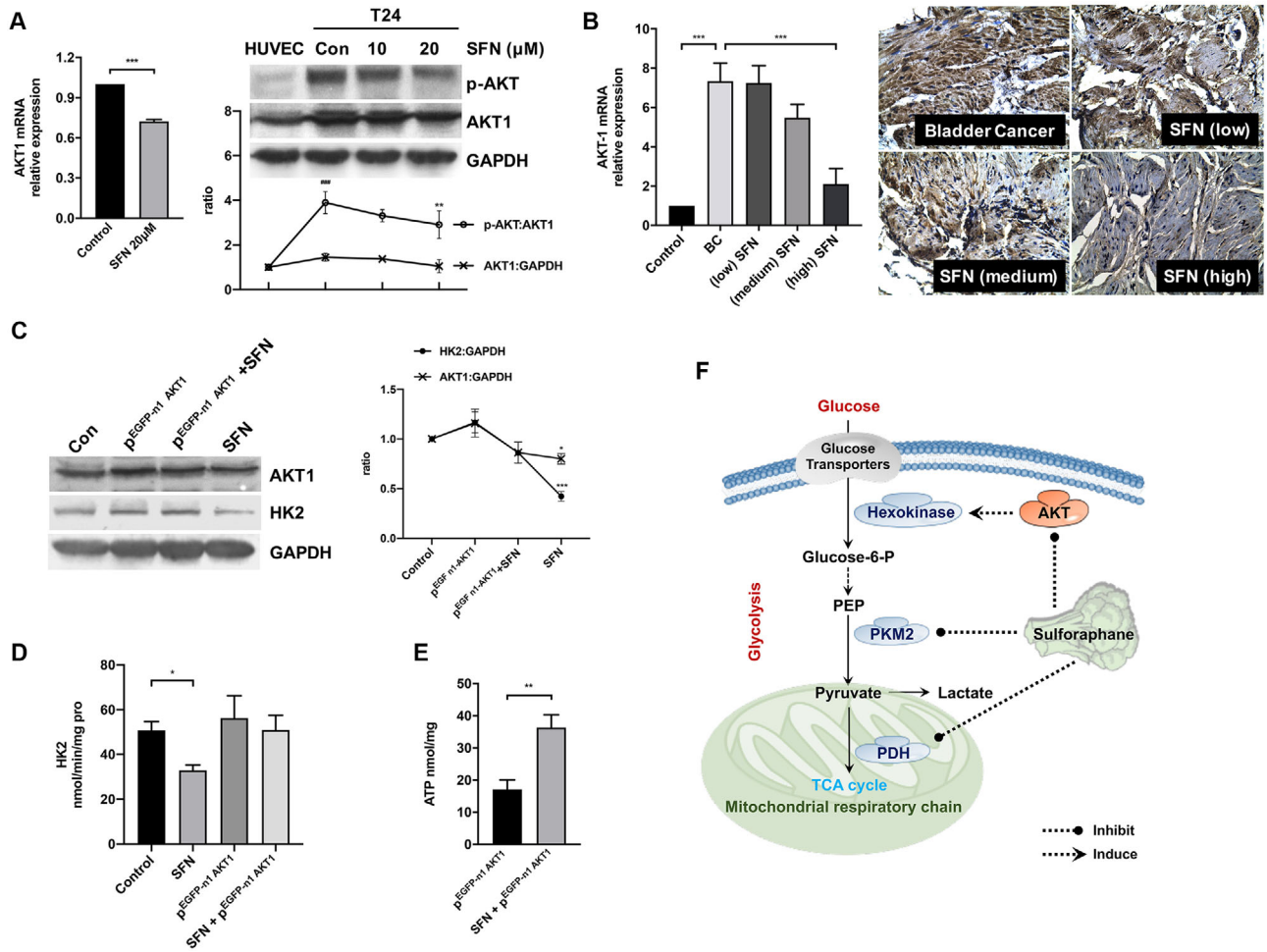

Figure 6. SFN reversed the dysregulation of glycolysis via the AKT1-HK2 axis. A) Cells were treated with or without SFN for 24 h before harvest. AKT1 mRNA expression in the left panel. Protein levels of p-AKT and AKT1 in the right panel and quantification at the bottom. B) qPCR analysis of AKT1 mRNA in bladder tissues (left panel); AKT1 expression by immunohistochemical staining (× 100 magnification, right panel). C) The protein levels of AKT1 and HK2 in AKT1-overexpressing T24 cells. D & E) HK2 activity (D) and ATP production (E) in AKT1-overexpressing T24 cells. F) Schematic mechanism of regulating glucose metabolism by SFN in human bladder cancer. Compared with the control group, $^{*}p < 0.05$, $^{**}p < 0.01$, $^{***}p < 0.001$; Compared with the HUVEC-negative control group, $^{\#\#\#}p < 0.001$.

could be a major contributor to high glycolytic flux. In the present study, SFN exhibited the strongest inhibitory effect on low-grade bladder cancer by blocking HK2 expression. The glycolysis in bladder tumors was aberrantly elevated by AKT1, a classic "Warburg kinase."[26] According to Neary et al., AKT inhibition promotes nuclear HK2 localization and glucose uptake in cervical cancer cells.[27] However, in human colorectal cancer cells, AKT suppression significantly decreased HK2 and the overexpression of AKT rescued the inhibitory effect, suggesting that AKT can effectively regulate glycolysis by inducing HK2 expression.[28] Consistently, SFN had a strong inhibitory effect on the p-AKT and HK2 protein in bladder cancer cells (especially in low-invasive UMUC3 cells), while the overexpression of AKT could strongly reverse the inhibitory effect. These findings also explained our previous bioenergetic analysis showing that SFN presented a stronger inhibition of ATP production in low-invasive cells. Coincidentally, our results demonstrated that the dysregulation of energy metabolism in low-grade patients (T1 stage) was stronger than that in high-grade patients (T2 stage). Taken together, we believe that SFN may have a better targeted improvement on energy metabolism in bladder cancer patients.

PKM2 presents as a glycolytic enzyme in the cytoplasm, while as a protein kinase in the nucleus which can promote tumorigenesis and progression through non-glycolytic metabolic regulation.[29] The upregulation of the nuclear-PKM2 level can facilitate tumor cell migration through activating STAT3 signaling pathway.[30] To our knowledge, studies about the effect of SFN on PKM2 expression in bladder tumor cells are still lacking. Interestingly, our work suggested that SFN strongly inhibited the expression of nuclear-PKM2 but not total-PKM2 protein in UMUC3 cells. Therefore, we speculated that SFN may also reverse bladder tumor progression through inhibiting nuclear-PKM2 expression, a non-glycolytic mechanism.

In conclusion, our work emphasized that the unique glucose metabolic abnormalities in T1 stage of the bladder cancer patients was the most obvious. SFN strongly downregulated the

glucose metabolism of bladder cancer cells in vitro and in vivo by blocking the AKT1-HK2 axis, especially in low-invasive UMUC3 cells. Therefore, targeting the specific metabolic type may provide more powerful therapeutic effectiveness. Based on the above, SFN is potentially a promising antineoplastic agent for bladder cancer patients with lower grades.

Supporting Information

Supporting Information is available from the Wiley Online Library or from the author.

Acknowledgements

The authors are grateful to Dr Christopher Dacosta (University of Glasgow) and Prof. Yongping Bao (University of East Anglia) for the critical reading of the manuscript. This study was supported by the National Natural Science Foundation of China (NSFC) (81773427).

Conflict of Interest

The authors declare no conflict of interest.

Author Contributions

L.H.: Data curation, Writing-Original draft preparation, Methodology; C.H.: Resources, Validation; S.Z.: Formal analysis; C.W.: Investigation, Visualization; M.R.: Resources; Y.S.: Conceptualization, Supervision, Writing-Reviewing and Editing.

Data Availability Statement

The data that supports the findings of this study are available in the supplementary material of this article.

Keywords

aerobic glycolysis, bladder cancer, glucose metabolism, glycolysis, sulforaphane

Received: August 5, 2021
Revised: September 26, 2021
Published online:

[1] Y. R. Lee, M. Chen, J. D. Lee, J. F. Zhang, S. Y. Lin, T. M. Fu, H. Chen, T. Ishikawa, S. Y. Chaing, J. Katon, Y. Zhang, Y. V. Shula, A. C. Bester, J. Fung, E. Monteleone, L. Wan, C. Shen, C. H. Hsu, A. Papa, J. G. Clohessy, J. T. Feldtein, S. Jain, H. Wu, L. Matesic, R. H. Chen, W. Wei, P. P. Pandolfi, *Science* **2019**, *364*, eaau0159.
[2] P. Soundararajan, J. S. Kim, *Molecules* **2018**, *23*, 2983.
[3] M. S. Jaman, M. A. Sayeed, *Breast Cancer* **2018**, *25*, 517.
[4] D. B. Nandini, R. S. Rao, B. S. Deepak, P. B. Reddy, *J Oral Maxillofac Pathol* **2020**, *24*, 405.
[5] A. Vanduchova, P. Anzenbacher, E. Anzenbacherova, *J Med Food* **2018**, *22*, 121.
[6] Y. Zhang, *Mutat Res* **2004**, *555*, 173.
[7] T. Li, G. R. Zirpoli, K. Guru, K. B. Moysich, Y. S. Zhang, C. B. Ambrosone, S. E. McCann, *Cancer Epidemiol Biomarkers Prev* **2010**, *19*, 1806.
[8] R. Hudlikar, L. Wang, R. Wu, S. Y. Li, R. Peter, A. Shannar, P. J. Chou, X. Liu, Z. J. Liu, H. D. Kuo, A. N. Kong, *Cancer Prev Res (Phila)* **2020**, *14*, 151.
[9] L. Huang, B. L. Li, C. X. He, Y. J. Zhao, X. L. Yang, B. Pang, X. H. Zhang, Y. J. Shan, *J Funct Foods* **2018**, *41*, 118.
[10] Y. Shan, L. Zhang, Y. Bao, B. Li, C. He, M. Gao, X. Feng, W. Xu, X. Zhang, S. Wang, *J. Nutr. Biochem.* **2013**, *24*, 1062.
[11] X. Luo, C. Cheng, Z. Tan, N. Li, Y. Cao, *Mol Cancer* **2017**, *16*, 76.
[12] M. P. Scholtes, A. R. Alberts, I. G. Iflé, P. Verhagen, T. Zuiverloon, *Int. J. Mol. Sci.* **2021**, *22*, 2832.
[13] X. Luo, C. Cheng, Z. Tan, N. Li, Y. Cao, *Mol Cancer* **2017**, *16*, 76.
[14] N. Putluri, A. Shojaie, V. T. Vasu, S. K. Vareed, A. Sreekumar, *Cancer Res.* **2011**, *71*, 7376.
[15] N. Bansal, A. Gupta, N. Mitash, P. S. Shakya, A. Mandhani, A. A. Mahdi, S. N. Sankhwar, S. K. Mandal, *J. Proteome Res.* **2013**, *12*, 5839.
[16] K. Dettmer, F. C. Vogl, A. P. Ritter, W. T. Zhu, *Electrophoresis* **2013**, *34*, 2836.
[17] P. Lei, S. C. Tian, C. Y. Teng, L. Huang, X. D. Liu, J. J. Wang, *Mol. Nutr. Food Res.* **2018**, *63*, 1800795.
[18] S. C. Tian, B. L. Li, P. Lei, X. Yang, Y. J. Shan, *Mol. Nutr. Food Res.* **2018**, *62*, 1700737.
[19] N. Ito, *Cancer Res.* **1976**, *36*, 2528.
[20] P. L. Ho, E. J. Lay, W. Jian, D. Parra, K. S. Chan, *Cancer Res.* **2012**, *72*, 3135.
[21] Y. Xie, X. Shi, K. Sheng, G. Han, W. Li, Q. Zhao, B. Jiang, J. Feng, J. Li, Y. Gu, *Mol. Med. Rep.* **2018**, *19*, 783.
[22] R. Liu, Y. Chen, G. Liu, C. Li, Y. Song, Z. Cao, W. Li, J. Hu, C. Lu, Y. Liu, *Cell Death Dis.* **2020**, *24*, 797.
[23] L. Schwartz, C. T. Supuran, K. O. Alfarouk, *Anticancer Agents Med Chem* **2017**, *17*, 164.
[24] P. B. Ancey, C. Contat, E. Meylan, *FEBS J.* **2018**, *285*, 2926.
[25] S. Ganapathy-Kanniappan, J. F. H. Geschwind, *Mol Cancer* **2013**, *12*, 152.
[26] V. R. Conde, P. F. Oliveira, A. R. Nunes, C. S. Rocha, E. Ramalhosa, J. A. Pereira, M. G. Alves, B. M. Silva, *Exp. Cell Res.* **2015**, *335*, 91.
[27] L. C. Neary, G. J. Pastorino, *J. Cell. Physiol.* **2013**, *228*, 1943.
[28] R. Courtnay, D. C. Ngo, N. Malik, K. Ververis, S. M. Tortorella, T. C. Karagiannis, *Mol. Biol. Rep.* **2015**, *42*, 841.
[29] K. B. Singh, E. R. Hahm, J. J. Alumkal, J. Joshi, M. L. Foley, T. K. Hitchens, *Carcinogenesis* **2019**, *40*, 1545.
[30] M. Tamada, M. Suematsu, H. Saya, *Clin. Cancer Res.* **2012**, *18*, 5554.

